COBEM2015

ABCM Associação Brasileira de Engenharia e Ciências Mecânicas

23rd ABCM International Congress of Mechanical Engineering
December 6-11, 2015, Rio de Janeiro, RJ, Brazil

SUPERCRITICAL SHOCK TUBE SIMULATION

Leandro Santos de Barros
Leonardo Santos de Brito Alves
Laboratory of Theoretical and Applied Mechanics — LMTA,
Department of Mechanical Engineering / PGMEC,
Universidade Federal Fluminense — UFF,
Rua Passo da Pátria 156, bloco E, sala 216, Niterói, RJ, 24210-240, Brazil
lsbarros@id.uff.br, leonardo.alves@mec.uff.br

Abstract. *In this paper we present a numerical code to simulate supercritical fluids using a finite difference scheme. Modelling fluids in the vicinity of its critical point has particular issues related to the characteristics of fluids under this condition, mainly the highly variable thermodynamic properties. Specifically, we perform a shock tube simulation, based on real-gas modelling in a Newtonian-Fourier fluid, using some cubic equation of state. Moreover, it is shown results for variable property to verify how this information can affect the numerical output.*

Keywords: *supercritical, numerical analyses, Navier-Stokes, mathematical modeling*

1. INTRODUCTION

On the last decades a growing interesting has appeared on the heat transfer phenomena in supercritical fluids, specially when a fluid is near critical thermodynamical point. This interest is mainly concerned about the so-called piston effect, the mechanism behind the fast energy transfer (Ball, 2000; Onuki *et al.*, 1990).

Fluids submitted to pressure and temperature above the critical point show characteristics similar to both liquids and gases and they are called supercritical fluids. Near the critical liquid-gas point the thermophysical properties are highly variable: for example, the compressibility factor becomes very large while thermal diffusivity goes to zero.

Despite studies date back century XIX (Berche *et al.*, 2009) and uncountable industrial applications during last decades (Kiran *et al.*, 2012), some experiments (Nitsche and Straub, 1987; Miura *et al.*, 2006) triggered new insights about thermo-mechanical interactions, opening a set of possible technological applications. To that become a reality, is very desirable numerical simulations tool to be developed and enhanced.

Arina (2004) has done tests in the case of the flow through a nozzle and the shock tube problem to show the reliability of the numerical finite volume scheme to support any equation of state. After him, (Terashima *et al.*, 2011; Jassim *et al.*, 2008; Barros, 2015) has presented their codes and used Arina's work as a test case to validate their codes. The shock tube is a simple and very ilustrative problem to test a shock capturing numerical scheme and able to test the capability of a code to reproduce the effect of a real gas.

We present a numerical scheme that is able to simulate a compressible fluid flow with heat transfer and able to adopt any equation of state. It is shown a high-order finite difference scheme. The results are for supercritical shock tube for variable thermodynamical property. It will be discussed some real gas effects. This investigation show how property variation can influence the output in such problems (highly variable pressure and temperature).

2. MATHEMATICAL FORMULATION

The one-dimensional Navier-Stokes equation – mass, momentum and energy conservation principles – can be written in conservative form as follow:

$$\frac{\partial \mathbf{q}}{\partial t} = \frac{\partial \mathbf{e}_\nu}{\partial x} - \frac{\partial \mathbf{e}_\iota}{\partial x} + \mathbf{s}, \tag{1}$$

where independents variables t and x represents the physical time and spatial dimension, respectively. The conservative dependent variables, viscous and inviscid fluxes are written, respectively, as:

$$\mathbf{q} = \{\rho, \quad \rho u, \quad \rho E\}, \quad \mathbf{e}_\iota = \{\rho u, \quad \rho u^2 + p, \quad (\rho E + p)u\}, \quad \mathbf{e}_\nu = \{0, \quad \mu^\star \frac{\partial u}{\partial x}, \quad u\,\mu^\star \frac{\partial u}{\partial x} + k\frac{\partial T}{\partial x}\} \tag{2}$$

and $\mathbf{s}$ is a source term. In the above definition, u stands for speed in x direction, $E = \varepsilon + u^2/2$ is the total energy per unit of mass, ε is internal energy per unit mass, μ is dynamic viscosity, λ is the second viscosity, $\mu^\star = (2\,\mu + \lambda)$, k is thermal conductivity, T is temperature and ρ is density. Stoke's hypotheses is assumed, i.e., $\lambda = -2/3\mu$.

The governing system (1) with a equation of state (EoS) is closed. Three equations of state have been considered. The ideal gas model (IG), the van der Waals model (VDW) and the Redlich-Kwong model (RK). The EoS's are written in dimensional variables,

$$p = \rho R T_{\text{ig}}, \tag{3a}$$

$$p = \frac{\rho R T_{\text{vdw}}}{1 - b_{\text{vdw}}\rho} - a_{\text{vdw}}\rho^2, \tag{3b}$$

$$p = \frac{\rho R T_{\text{rk}}}{1 - b_{\text{rk}}\rho} - \frac{a_{\text{rk}}\rho^2}{\sqrt{T_{\text{rk}}}(1 + b_{\text{rk}}\rho)}, \tag{3c}$$

Given that pressure and density are the input (initial condition), the temperature and the internal energy is EoS-dependent, given by:

$$\varepsilon_{\text{ig}} = c_v T, \tag{4a}$$

$$\varepsilon_{\text{vdw}} = c_v T - a_{\text{vdw}}\rho, \tag{4b}$$

$$\varepsilon_{\text{rk}} = c_v T - \frac{3}{2}\frac{a_{\text{rk}}}{b_{\text{rk}}}\frac{1}{\sqrt{T}}\log(1 + b_{\text{rk}}\rho), \tag{4c}$$

where R is the specific gas constant, c_v is the volume constant specific heat. Moreover, all the constants above are obtained from the critical pressure, density and temperature (p_c, ρ_c, T_c):

$$a_{\text{vdw}} = 3p_c/\rho_c^2, \qquad b_{\text{vdw}} = 1/(3\rho_c), \tag{5a}$$

$$a_{\text{rk}} = 0.42748\, R^2\, T_c^{2.5}/p_c, \qquad b_{\text{rk}} = 0.08664\, R\, T_c/p_c. \tag{5b}$$

As we are solving the shock tube problem, the viscous and source terms are neglected in our code.

2.1 Space discretization

The spatial discretizaton is generally managed acording to the fluxes's nature. For viscous fluxes, a conservative central discretization is appropriate while for the inviscid fluxes a upwind discretization is necessary (Hirsch, 1988). In order to properly implement the inviscid spatial discretization, we employed a Steger and Warming (1981) flux vector splitting, based on a wave speed, extended to real gases. We split the fluxes in this way,

$$\mathbf{e}_\iota = \mathbf{e}_\iota^+ + \mathbf{e}_\iota^-, \tag{6}$$

which is achieved through the separation of the wave speeds or eigenvalues. Wave speed splitting allows positive and negative characteristics to be separated for an appropriate upwind discretization. For an ideal gas it can be done easily just noticing that:

$$\mathbf{e}_\iota = \mathbf{A}\,\mathbf{q}, \qquad \mathbf{A} \equiv \frac{\partial \mathbf{e}}{\partial \mathbf{q}}, \qquad \mathbf{e}_\iota^\pm = \mathbf{A}^\pm\,\mathbf{q}, \qquad \text{and} \qquad \mathbf{A}^\pm \equiv \mathbf{M_A}\,\mathbf{\Lambda}^\pm\,\mathbf{M_A^{-1}}, \tag{7}$$

where $\mathbf{\Lambda}$ is the diagonal eigenvalues matrix with $\lambda_i^+ \geq 0$ and $\lambda_i^- < 0$ and the matrix $\mathbf{M_A}$ is defined as the eigenvectors matrix associated with $\mathbf{A}$. If the pressure of a gas does not depends linearly on ρ, equation (7) is not true. We employed the methodology for real gases developed by Liou *et al.* (1990). In order to explain the methodogy, note that the matrix $\mathbf{A}$ can be written as a function of $\mathbf{q}$ and $\mathbf{j}^\star$, where:

$$\mathbf{j}^\star = \Big\{p_\rho, \quad p_\varepsilon\Big\}, \qquad p_\rho \equiv \left(\frac{\partial p}{\partial \rho}\right)_\varepsilon \qquad \text{and} \qquad p_\varepsilon \equiv \left(\frac{\partial p}{\partial \varepsilon}\right)_\rho. \tag{8}$$

The matrix $\mathbf{A}$ is decomposed in two parts, $\mathbf{A} = \mathbf{A}_\varepsilon + \mathbf{A}_\rho$, where the matrix $\mathbf{A}_\varepsilon$ contains the derivative p_ε while $\mathbf{A}_\rho$ contains the derivative p_ρ:

$$\mathbf{A}_\varepsilon = \begin{pmatrix} 0 & 1 & 0 \\ -u^2\,(2 - p_\varepsilon/\rho)2 + (p - p_\varepsilon\,\varepsilon)/\rho & u\,(2 - p_\varepsilon/\rho) & p_\varepsilon/\rho \\ u\,[-H + u^2\,p_\varepsilon/2\,\rho + (p - p_\varepsilon\,\varepsilon)/\rho] & H - u^2\,p_\varepsilon/\rho & u\,(1 + p_\varepsilon/\rho) \end{pmatrix}, \tag{9}$$

and

$$\mathbf{A}_\rho = \begin{pmatrix} 0 & 0 & 0 \\ p_\rho - p/\rho & 0 & 0 \\ u\,(p_\rho - p/\rho) & 0 & 0 \end{pmatrix}, \tag{10}$$

where $H \equiv E + p/\rho$ is the total enthalpy per unit mass. The eigenvalues dictate the appropriate discretization scheme. For each matrix discussed above, the eigenvalues of which one are:

$$\lambda(\mathbf{A}) = (u - a,\, u,\, u + a), \tag{11a}$$
$$\lambda(\mathbf{A}_\varepsilon) = (u - a_\varepsilon,\, u,\, u + a_\varepsilon), \tag{11b}$$
$$\lambda(\mathbf{A}_\rho) = (0,\, 0,\, 0), \tag{11c}$$

where $a_\varepsilon = p\,(p_\varepsilon/\rho + 1) = a^2 - (p_\rho - p/\rho)$. Then the matrixes $\mathbf{A}$ and $\mathbf{A}_\varepsilon$ possess a set of eigenvectors.This implies that the terms associated to $\mathbf{A}_\rho$ has no preferential direction. The fluxes can be written in this form:

$$\mathbf{e}_\iota = \mathbf{e}_\iota^{\mathrm{IG}} + \mathbf{e}_\iota^\star, \tag{12}$$

where a upwind discretization is used for the first term while a centered discretization to the last one, and

$$\mathbf{e}_\iota^{\mathrm{IG}} = \mathbf{A}\,\mathbf{q}, \tag{13a}$$
$$\mathbf{e}_\iota^\star = \mathbf{A}_\rho\,\mathbf{q}, \tag{13b}$$

and one can write:

$$\mathbf{e}_\iota^{\mathrm{IG}\pm} = \mathbf{A}^\pm\mathbf{q}, \tag{14a}$$
$$\mathbf{e}_\iota^\pm = \mathbf{e}_\iota^{\mathrm{IG}\pm} + \frac{1}{2}\mathbf{e}_\iota^\star. \tag{14b}$$

To use a high order *upwind* scheme is necessary to adopt a Total Variation Diminishing methodology (Moraes *et al.*, 2012). The minmod limiter has been implemented to prevent oscillations around discontinuities (Hirsch, 1988).

2.2 Time discretization

It was implemented a second order temporal discretization with two stages. A Strong Stability Preserving Runge-Kutta (SSPRK) methodology (Moraes *et al.*, 2012). To describe the methodology, suppose a Partial Differential Equation (PDE) below:

$$u_t = f(u)_x, \tag{15}$$

where the index denote partial derivatives and u is a function of x and t. Let $F(u)$ be a spatial discretização of $f(u)_x$. So, the methodology is written as:

$$u^{(1)} = u^n + \Delta t \cdot F(u^n), \tag{16a}$$
$$u^{(2)} = \frac{1}{2}\cdot(u^n + u^{(1)}) + \frac{1}{2}\cdot\Delta t\cdot F(u^{(1)}), \tag{16b}$$
$$u^{n+1} = u^{(2)}, \tag{16c}$$

where n means numerical time.

3. NUMERICAL TEST

The purpose of the first numerical experiment is to test the numerical scheme, with the different EoS. Specifically, we want to verify the capability of the scheme in capturing flow discontinuities. The numerical solutions are compared with respect to the ideal gas case, for which the original numerical algorithms have been devised and optimized. The shock tube is an important test case to asses the effectiveness of the real gas methodology. We considered two shock tube problems similar to the proposed one by Sod (1978).

The problem simulated is known as shock tube, the inviscid Riemann problem, formed by a long tube with a thin diaphragm separating two states. The initial state is two uniform regions with p_1 (left) > p_2 (right). The tube length is L and the diaphragm is placed at the middle of the tube. At $t = 0$ the diaphragm is removed to produce a shock and a contact discontinuity propagating down the tube into the gas on the low pressure side, and an expansion wave moves into the high pressure gas.

For classical shock tube, the pressure p_1 = 10^5 Pa, density $\rho_1 = 1\mathrm{kg/m^3}$; on the other side, the fluid is p_2 = 10^4 Pa, $\rho_2 = 0.125\mathrm{kg/m^3}$. To test the impact of a EoS and analyse the influence of property variation, a supercritical shock tube is simulated with CO_2 for: p_1 = 10^5 Pa, $\rho_1 = 1\mathrm{kg/m^3}$; p_2 = 10^4 Pa, $\rho_2 = 0.125\mathrm{kg/m^3}$. As usual, the classical boundary condition is given as:

$$\frac{\partial p}{\partial x} = 0, \qquad \frac{\partial \rho}{\partial x} = 0, \qquad u = 0, \qquad \text{for} \quad x = 0 \quad \text{and} \quad x = L \tag{17}$$

4. DISCUSSION AND RESULTS

The first problem was simulated with a mesh $N_x = 401$ points with the fluid in the region whose compressibility factor $Z = 1$, ie, superheated region, where the fluid can be considered an ideal gas. In this region, all the results, indepently of EoS, should recover the ideal gas results. These results were validated to the exact solution.

In the second simulation, was performed with mesh of $N_x = 501$ and $N_x = 1501$ points and compared with Arina's results. For this problem, supercritical shock tube, two simulations were made: the first one using the same parameters used by Arina and the second one for variable properties; the input data was the initial condition, R and the critical constants (pressure, density and temperature).

4.1 Validation and Order Verification

Figure 1 shows the results for pressure profile at $t = 10^{-2}s$ for the classical shock tube for each EoS. All results recover the ideal gas case. Figure 2 shows the density profile. These preliminaries tests show that this code can handle with a non-ideal gas EoS.

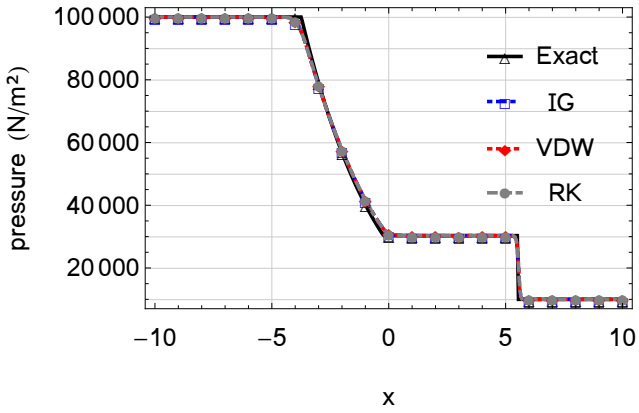

Figure 1. Pressure in a classical shock tube, $N_x = 401$, $\Delta t = \text{CFL} \cdot \Delta x/340$, CFL = 0.04.

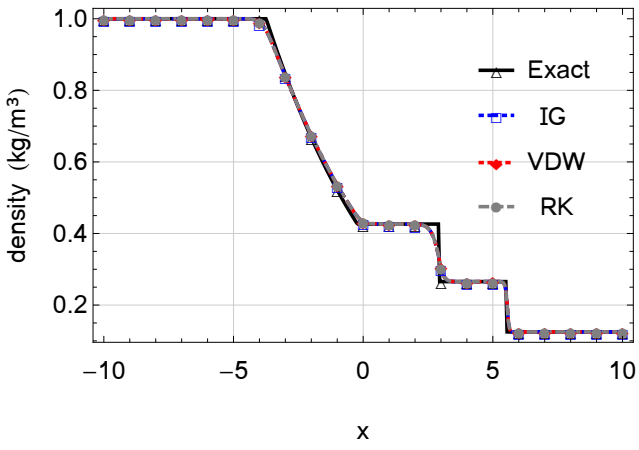

Figure 2. Density in a classical shock tube, $N_x = 401$, $\Delta t = \text{CFL} \cdot \Delta x/340$, CFL = 0.04.

The table 1 report the calculated numerical spatial order. The calculed one is a bit less than the theorical order. The table 2 shows the temporal order, based on the maximum density error. All the computations have been performed on a Intel Core i5 processor, with 2.3 GHz.

TVD: $O(\Delta x^2)$		
N_x	error $(\mathrm{kg/m^3})$	rate
51	1.75122×10^{-10}	–
101	2.52658×10^{-11}	2.7931
201	7.00406×10^{-12}	1.85092
401	2.06846×10^{-12}	1.75964
801	5.78537×10^{-13}	1.83807

Table 1: Spatial order analyses. Second-order method with TVD and minmod flux limiter.

SSP: $O(\Delta t^2)$, $\Delta t_{\mathrm{ref}} = 6.0 \times 10^{-7}\mathrm{s}$		
$\Delta t/\Delta t_{\mathrm{ref}}$	error $(\mathrm{kg/m^3})$	rate
1/2	5.82978×10^{-13}	–
1/4	1.55986×10^{-13}	1.90202
1/8	3.98570×10^{-14}	1.96851
1/16	1.13243×10^{-14}	1.81541

Table 2: Temporal order analyses. Second-order SSPRK method.

Figure 3 shows a density profile for the shock tube. The exact solution is the analytical one given the ideal gas assumption. Figure 4 is a density profile for van der Waals and Redlich-Kwong models. The present simulation was done for constant property assumption (and $N_x = 1501$), similarly as Arina ($N_x = 501$). This code can reproduce these results very well.

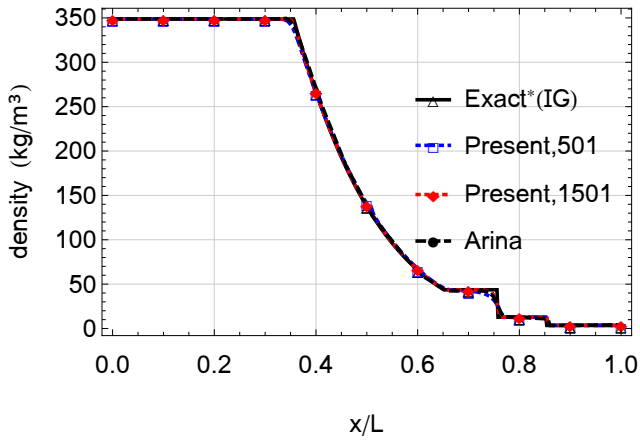

Figure 3. Density in a supercritical shock tube. Exact solution under IG hypotheses.

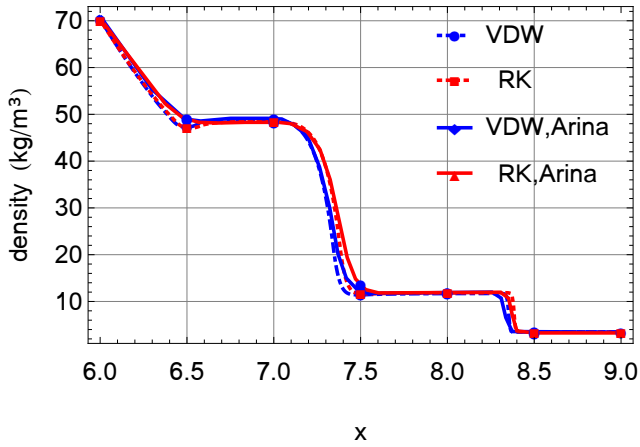

Figure 4. Density for the van der Waals (VDW), Redlich-Kwong (RK) equation of state, for constant property: supercritical shock tube; $N_x = 1501$, $\Delta t = 0.001/c_0$, $c_0 = \sqrt{1,3 \times R/T_c}$, $x_L = 0$, $x_R = 10$, minmod flux limiter. Arina (2004) solution for $N_x = 501$.

5. Results for Property Variation

Figure 5 shows the results for pressure and density in a supercritical shock tube. Arina's results and the present results for varible property are shown, where the latter one predicts a faster expansion fan with respect to the Arina's results.

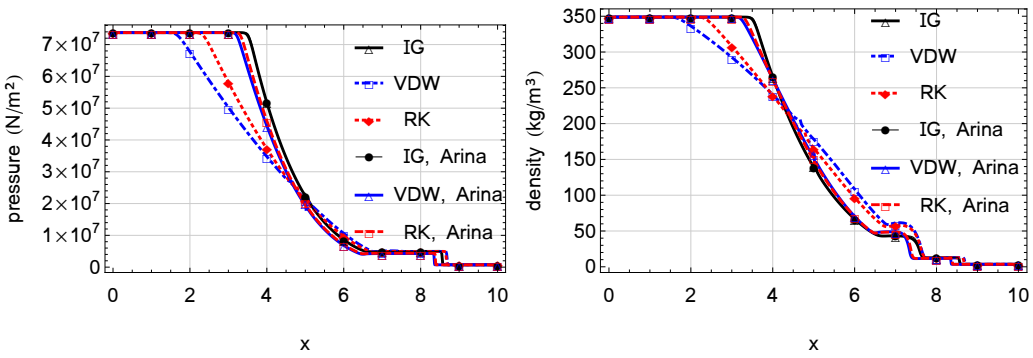

Figure 5. Pressure and density, supercritical shock tube. $N_x = 1501$, $\Delta t = 0.001/c_0$, $c_0 = \sqrt{1,3 \times R/T_c}$.

The small flow differences around the discontinuities predicted by the real gas models, can be seen in the enlargement displayed in figure 6. Arina's results are for constant property.

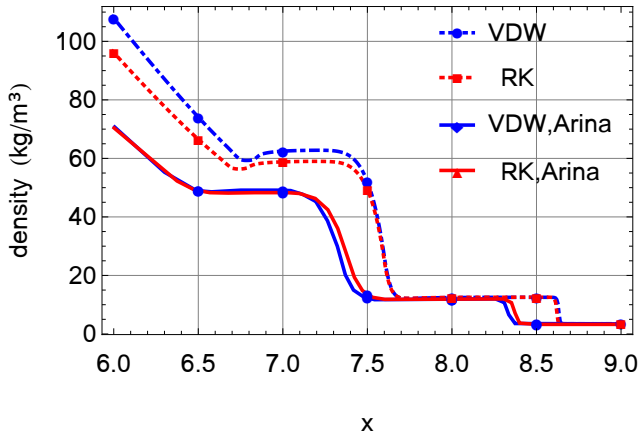

Figure 6. Density for van der Waals (VDW) and Redlich-Kwong (RK) models. Comparison betwen Arina's solution and a property variation solution. supercritical shock tube; $N_x = 1501$, $\Delta t = 0.001/c_0$, $c_0 = \sqrt{1,3 \times R/T_c}$, $x_L = 0$, $x_R = 10$. Arina's solution for $N_x = 501$.

6. CONCLUSION

We have presented a numerical scheme for the solution of a supercritical fluid flow in tube shock. The methodology is based on the Steager-Warming flux-split difference scheme for real-gas and a second-order accurate Runge-Kutta explicit scheme in time. The independence of the numerical algorithm upon the specific structure of the real gas equation of state is the main advantage.

It was considered two equations of state describing the thermodynamic behavior of the fluid near the critical point. The van der Waals model and the Redlich-Kwong model. The numerical simulations obtained with the two state equations, in the case of the flow through a one-dimensional shock-tube problem, assess the ability of the explicit scheme in capturing flow discontinuities (shocks and contact discontinuities).

The effect of variable property in a supercritical shock tube is also investigated. The numerical solutions are in agreement with the classical results in the literature for constant property. A higher computational cost for variable property case is seen and a significantly different wave form is observed.

We focused on one-dimensional flows, but the approach may be directly extended to multidimensional geometries.

7. ACKNOWLEDGEMENTS

The authors would like to acknowledge the financial support received by FAPERJ, CNPq and CAPES.

8. REFERENCES

Arina, R., 2004. "Numerical Simulation of Near-Critical Fluids". *Applied Numerical Mathematics*, Vol. 51, No. 4, pp. 409–426.

Ball, P., 2000. "Pump up the volume". 9 Jun. 2015 <http://www.nature.com/news/2000/000508/full/news000511-3.html>.

Barros, L.S.d., 2015. *Alguns Efeitos em Ondas Termoacústicas devido a Fortes Variações de Pressão e Temperatura*. Master's thesis, Universidade Federal Fluminense.

Berche, B., Henkel, M. and Kenna, R., 2009. "Critical Phenomena: 150 Years Since Cagniard de La Tour". *Revista Brasileira de Ensino de Física*, Vol. 31.

Hirsch, C., 1988. *Numerical Computation of Internal and External Flows, Vol. 2 Computational Methods for Inviscid and Viscous Flows*. Wiley, Chichester.

Jassim, E., Abdi, M.A. and Muzychka, Y., 2008. "Computational Fluid Dynamics Study for Flow of Natural Gas Through High-Pressure Supersonic Nozzles: Part 1. Real Gas Effects and Shockwave". *Petroleum Science and Technology*, Vol. 26, No. 15, pp. 1757–1772.

Kiran, E., Debenedetti, P.G. and Peters, C.J., 2012. *Supercritical Fluids: Fundamentals and Applications*, Vol. 366. Springer Science & Business Media.

Liou, M.S., Van Leer, B. and Shuen, J.S., 1990. "Splitting of Inviscid Fluxes for Real Gases". *Journal of Computational Physics*, Vol. 87, No. 1, pp. 1–24.

Miura, Y., Yoshihara, S., Ohnishi, M., Honda, K., Matsumoto, M., Kawai, J., Ishikawa, M., Kobayashi, H. and Onuki, A., 2006. "High-Speed Observation of the Piston Effect Near the Gas-Liquid Critical Point". *Physical Review E*, Vol. 74, No. 1, p. 010101.

Moraes, G.D., Medeiros, F.E.L.D. and Alves, L.S.d.B., 2012. "Analysis of Strong Stability Preserving Runge-Kutta Methods". In *CONEM 2012*.

Nitsche, K. and Straub, J., 1987. "The Critical Hump of Cv Under Microgravity, Results From D-Spacelab Experiment "WärmekapazitäT"". In *Proceedings of the 6th European Symp. on Material Sci. under Microgravity Conditions, ESA SP-256*. p. 109.

Onuki, A., Hao, H. and Ferrell, R.A., 1990. "Fast Adiabatic Equilibration in a Single-Component Fluid Near the Liquid-Vapor Critical Point". *Physical Review A*, Vol. 41, No. 4, pp. 2256–2259.

Sod, G., 1978. "A Survey of Several Finite Difference Methods for Systems of Nonlinear Hyperbolic Conservation Laws". *Journal of Computational Physics*, Vol. 31, pp. 1–31.

Steger, J.L. and Warming, R.F., 1981. "Flux Vector Splitting of the Inviscid Gasdynamic Equations with Application to Finite-Difference Methods". *Journal of Computational Physics*, Vol. 40, No. 2, pp. 263–293.

Terashima, H., Kawai, S. and Yamanishi, N., 2011. "High-Resolution Numerical Method for Supercritical Flows with Large Density Variations". *AIAA journal*, Vol. 49, No. 12, pp. 2658–2672.

9. RESPONSIBILITY NOTICE

The authors are the only responsible for the printed material included in this paper.